In Situ Examination of the Structure of Model Reversed-Phase Chromatographic Interfaces by Sum-Frequency Generation Spectroscopy

Matthew C. Henry, Lauren K. Wolf,† and Marie C. Messmer*

Department of Chemistry, Lehigh University, 7 Asa Drive, Bethlehem, Pennsylvania 18015

Received: August 26, 2002

Model reversed-phase chromatographic interfacial systems were examined using sum-frequency generation (SFG) spectroscopy to study the effect of solvent on the structure and conformation of the stationary phase. Monolayers formed from mixed C_{18} and C_1 alkysilanes (both polymeric octadecyltrichlorosilane-methyl trichlorosilane mixed monolayers and monomeric octadecyldimethylchlorosilane-trimethylchlorosilane mixed monolayers) on fused silica were examined in contact with air, deuterated acetonitrile (CD_3CN), D_2O, and mixtures of CD_3CN and D_2O. When mixed composition (C_{18} and C_1) monolayers were examined, significant disorder was observed in the alkyl chains for all solvents examined at intermediate alkyl chain densities for the polymeric materials, and at all chain densities for the monomeric materials. Maximum order for intermediate polymeric chain densities was found to occur in contact with 40−50 vol % D_2O solutions. These results indicate that solvent microheterogeneity has a large effect on alkyl chain order.

Introduction

Chromatographic interfaces are complex systems involving many variables that control separation. One current challenge in understanding solute retention in chromatographic systems is understanding the complex interaction between solvent and stationary phase. The importance of stationary phase characteristics such as alkyl chain density, solvent penetration, stationary phase ordering, and residual silanol effects on stationary phase properties are still a broad area of investigation.[1−8] Binary solvent solutions such as those used in gradient elution pose a particular challenge because solvent microheterogeneity, solvent layering, and solvent-induced stationary phase structural changes make determining the relative contribution of solvent and stationary phase effects difficult.

Much evidence exists to support the essential role of the stationary phase in elution with binary solutions. Thermodynamic measurements have shown that changing acetonitrile−water composition changes the entropy of solute "transfer".[1] This change is attributed to formation of highly ordered stationary phases at high acetonitrile concentrations. It is believed that an ordered stationary phase can reduce the entropy of transfer to an extent that retention becomes enthalpically driven.[2] When the stationary phase is ordered, the entropic cost can be equal for adsorption and desorption of an analyte. Studies of interphase regions using deuterium NMR have shown that mobile phase composition determines the structure of the stationary phase.[3] NMR has shown that water does not associate strongly with alkyl chains, but acetonitrile does. Acetonitrile-enriched regions are present even at low mole fractions due to the microheterogeneous environment of binary acetonitrile−water mixtures.[9]

Acetonitrile−water mixtures are commonly used in reversed-phase liquid chromatography. Despite their ubiquity, the behavior of acetonitrile−water solutions in chromatographic systems is not simple. A solution of acetonitrile and water is a microheterogeneous mix of acetonitrile-rich and water-rich regions. Microheterogeneity has also been observed in actual chromatographic systems,[9] and computationally using Kirkwood−Buff integrals[10,11] and quasi-lattice quasi-crystal theory.[10,12] Mixtures of acetonitrile and water have been shown to exhibit this heterogeneity at the air−water interface.[13] In experimental[14] and computational studies,[15] the viscosity of acetonitrile−water solutions has been shown to exhibit a maximum at an acetonitrile mole fraction of about 0.15, although acetonitrile is less viscous than water. Presumably, such behavior should also occur at the solution-stationary phase interface. Under these conditions, the stationary phase experiences a solvent environment quite different from the bulk solution.

Studies of the interphase between solvent and stationary phase do not present an unambiguous picture of the interphase response to changing interface solvent conditions. Previous in situ studies of the alkyl stationary phase using surface enhanced Raman spectroscopy have concluded that little conformational change in the interphase occurs when a polar solvent is added.[4] Fluorescence experiments have shown that as organic modifiers are added to the mobile phase, bonded alkyl chains evolve from a collapsed "oil drop" to an extended "brush-like" configuration.[5,6] Solid-state NMR studies by Albert and co-workers support this hypothesis as well.[7] However, recent Raman spectroscopic studies by Doyle et al.[8] show that conformational changes observed between aqueous and organic environments did not produce a distinct collapsed/extended alkyl chain transition, but were subtler.

Solvatochromic studies on the polarity of the stationary phase by Rutan and Harris indicate that the polarity of the stationary phase is modified considerably by intercalated solvent molecules.[16] Carr and co-workers found that typical C_{18} stationary phases are more similar to 2-propanol than bulk liquid hexadecane.[17] On the basis of these studies, the stationary phase must

† Current address: Department of Chemistry, Boston University, 590 Commonwealth Ave., Boston, MA 02215-2521.

10.1021/jp021984c CCC: $25.00
Published on Web 03/05/2003

be seen as a place where physical structure and chemical properties are intimately associated with solvent composition.

The nature of the interphase is also dependent on the chemical nature of the C_{18} chains. Though most commercial stationary phase materials are made from monomeric octadecyldimethylsilane, Wirth and co-workers have created stable chromatographic surfaces with mixed self-assembled monolayers (SAMs) of "horizontally polymerized" trifunctional alkyl silanes at the silica surface.[18,19] These stationary phases have shown superior chromatographic performance for the analysis of polyaromatic hydrocarbons[20] and superior stability at low pH.[21,22]

To further explore the structure of stationary phases in mixed solvent environments, we examined both monomeric and polymeric interfaces in air and CD_3CN-D_2O solution using sum-frequency generation spectroscopy. Sum-frequency generation (SFG) spectroscopy is a powerful surface analysis tool, proven to be invaluable in studying molecular structure at interfaces obscured by adjacent bulk phases. Interfaces that have been successfully explored include gas−liquid, liquid−liquid, liquid−solid, and gas−solid.[23] The forbidden nature of the process in bulk isotropic media (in the electric dipole approximation) permits in situ examination of the monolayer-solution interphase.

Experimental Section

Reagents. Octadecyltrichlorosilane (95%), octadecyldimethylchlorosilane (95%), trimethylchlorosilane (95%), and methyltrichlorosilane (99%) obtained from Aldrich were used without further purification. Hexadecane (99+%), squalane (99%), and carbon tetrachloride (99.9+%) were used as received from Aldrich. Sulfuric acid and hydrogen peroxide (analytical grade) were from EM Science. Acetone and isopropyl alcohol (HPLC and ACS grade, respectively) were from Pharmco Products. Methanol (Optima Grade, Fisher) was used as received. Deuterated acetonitrile (99.9 atom % D) and D_2O (99.9 atom %D) were from Aldrich.

Substrate Preparation. Fused silica slides (50 × 25 × 1 mm), from ChemGlass, Inc., were swabbed and rinsed with isopropyl alcohol then distilled water. Slides were dried under nitrogen and immersed in "piranha solution" (7:3 concentrated H_2SO_4/30% H_2O_2) for 1 h. **WARNING:** *Piranha solution should be kept out of contact with oxidizable organic material. It is a highly reactive mixture and severely exothermic during reaction.* After 1 h, the slides were removed and thoroughly rinsed with distilled water and dried with nitrogen. The RMS roughness of the bare fused silica slide after piranha treatment was ∼1.7 nm by atomic force microscopy (AFM).

Monolayer Formation. Before deposition, each slide was equilibrated over a saturated $Ca(NO_3)_2$ aqueous solution for 1 h to ensure a consistent relative humidity of 64 ± 1%. The constant relative humidity ensures that all slides have similar amounts of adsorbed water. A deposition mixture of octadecyltrichlorosilane and methyltrichlorosilane (ODS monolayers) or octadecyldimethylchlorosilane and trimethylchlorosilane (ODMS monolayers) at a total concentration of 20 mM in hexadecane and carbon tetrachloride (4:1 by volume) solution was prepared. Once surface humidification was complete, each slide was placed in a silanized reaction cell. Deposition solution was added to the cell, and the mixture was allowed to stand for 4 h. After reaction, slides were removed, rinsed with acetone and methanol, swabbed lightly to remove excess material, and rinsed again with copious amounts of the same solvents. Finally, each sample was dried under nitrogen, placed in an oven at 70 °C for 30 min, and stored in a sealed vial. The ODMS samples were prepared using the procedure of Fadeev and McCarthy[24] for 72 h at room temperature.

TABLE 1: C_{18} (ODS) and C_1 (MS) Concentrations in Solutions and Monolayers Used

[ODS], mM	[MS], mM	% ODS (bulk)	% ODS by XPS	log (C_{18}/C_1)	C_{18} density, μmol/m^2
20.00	0.0	100	100	∞	8.0
19.71	0.26	98.7	98.7	1.9	7.9
19.50	0.55	97.2	97.3	1.6	7.8
19.10	0.85	95.7	95.7	1.4	7.7
18.79	1.23	93.8	93.9	1.2	7.5
18.28	1.67	91.5	91.6	1.0	7.3
16.86	3.07	84.2	84.6	0.7	6.8
13.41	6.47	67.2	67.4	0.3	5.3
10.36	9.54	52.0	52.1	0.0	4.2
4.88	14.99	24.2	24.5	−0.5	2.0
2.34	17.72	11.8	11.6	−0.9	0.9
0	20.00	0.0	0.0	−∞	0.0

Contact Angle Measurements. Before analysis, each sample was dried at 70 °C for 30 min. A computer driven goiniometer (Connelly Applied Research) was used to establish the drops and evaluate their contact angles. Probe liquid was pumped onto the surface at 3 μL/s to form a ∼5 mm diameter sessile drop. The liquid was then advanced at 1 μL/s five times for each of three drops. The pump was stopped after each advance and images of the drops were captured after a 60 s equilibration time. Contact angles were determined on both sides of the drop using a subpixel interpolation method. Thirty measurements were averaged for each sample with water and hexadecane. Due to the relatively high viscosity of squalane,[25] squalane contact angles were determined from a static drop deposited on a slide and equilibrated for three minutes before measurement. A goiniometer was used to determine the average of eight contact angles for each slide.

X-ray Photoelectron Spectroscopic Measurements. X-ray photoelectron spectroscopy (XPS) data were acquired with a Scienta ESCA 300 using monochromatic Al Kα X-rays. The analysis area of each sample was approximately 0.8 mm^2, with a pass energy 150.0 eV and a 90° takeoff angle. The chamber pressure was approximately 5 × 10^{-9} Torr. Ten scans of the C1s region were taken for carbon and five scans of the Si2p region were taken for silicon. All spectra were fitted using a Voigt function with linear background correction in the Scienta software. Integrated peak areas were divided by atomic sensitivity factors, provided by the Scienta software. Monolayer composition was calculated as described previously.[26] After 4 h of equilibration in solution, the surface composition of the ODS samples was nearly identical to the solution composition. The various surface compositions are shown in Table 1. Chain densities are calculated assuming a maximum possible chain density on well humidified silica of 8.0 μmol/m^2 for ODS. This figure is based both on the density of silanols on the surface[27] and on the maximum chain density of crystalline octadecane.[28]

The ODMS samples were allowed to react for 72 h at room temperature. With the extended reaction time, the surface composition of C_1 and C_{18} chains is assumed to parallel the solution composition in a manner similar to the ODS samples. The maximum density of ODMS on the surface was taken to be 4.5 μmol/m^2.[29]

Sum-Frequency Spectroscopic Measurements. The sum-frequency generation equipment is described in detail elsewhere.[30] Briefly, a lithium niobate ($LiNbO_3$) optical parametric oscillator is pumped with a Surelite I (Continuum) Nd^{3+}:YAG laser using relay imaging. Tunable infrared light is generated between 2600 and 3200 cm^{-1} (3.1−3.8 μm) with a pulse width

of 7 ns. Wavelength is calibrated with a polystyrene reference standard. The 532 nm beam used is generated in a potassium dihydrogen phosphate (KDP) crystal. Polarization of the IR beam is controlled with a Soleil-Babinet compensator. Sum-frequency spectra were obtained in the total internal reflection geometry in which both the tunable infrared and the 532 nm light approach the interface through the quartz substrate. Infrared and 532 nm beams are passed through a coupling prism and index-matching liquid to intersect on the fused silica substrate. Sum-frequency light is collected and passed through collimating optics, absorptive, interference, holographic filters, and a Glan-Taylor polarizer. Signal is detected with a photomultiplier tube, preamplifier, and gated electronics. The average of 200 laser shots for each data point was acquired using a custom LabVIEW program. Sampling size on the surface was approximately 200 μm in diameter, determined by the IR spot size. Each spectrum is representative of spectra taken at several places on the sample.

Orientation of molecules at the surface is studied by changing polarization of the incident light beams. Spectra can be taken by selecting *s*-polarized output, and using *s*-polarized 532 nm and *p*-polarized IR (*ssp* combination) to probe molecules with IR transition dipole moment components normal to the surface. For IR transition dipoles parallel to the surface, the *sps* combination is used, with *s*-polarized sum frequency, *p* polarized 532 nm, and *s*-polarized IR.

Two parameters based on sum-frequency intensity ratios are calculated from the integrated peak intensities of the SFG spectra. The first is the sum-frequency intensity ratio, the ratio of the CH_3 symmetric stretch peak at approximately 2872 cm^{-1} to the CH_2 symmetric stretch peak at 2840 cm^{-1} (I_{CH_3}/I_{CH_2}). This ratio indicates the degree of order in the alkyl chains. The second parameter is the ratio of the CH_3 symmetric stretch *ssp* peak intensity to the CH_3 symmetric stretch *sps* peak intensity (I_{ssp}/I_{sps}). A change in the ratio indicates reorientation of CH_3 groups at the surface.

The MS component of mixed monolayers shows a CH_3 symmetric stretch peak at 2916 cm^{-1}. The CH_3 group of MS is directly attached to silicon, producing a blue shift relative to the terminal CH_3 group of ODS. Peak intensities of ODS can be quantified without interference from the MS CH_3 peak.

Due to the small difference in refractive index of D_2O and CD_3CN (less than 0.01), the critical angle for the 532 nm beam does not vary greatly with solution composition. Results were obtained without altering the experimental geometry for a series of CD_3CN-D_2O solutions. To account for changes in refractive index in the IR region, the IR beam was adjusted so that its incidence angle was above the critical angle for all compositions and wavelengths studied. To further reduce any refractive index effects, the intensities of the spectra were normalized by the intensity of a C_1 MS monolayer run under the same conditions. The CH_3 groups in the MS monolayer cannot undergo reorientation, because the CH_3 groups bond directly to silicon.

Results and Discussion

Contact Angle Measurements. In Figure 1A, hexadecane and squalane show minimum contact angles of 0° and 15°, respectively, at a $\log(C_{18}/C_1)$ ratio of 0.0 (4.2 μmol/m^2 ODS). This observation is consistent with a surface composed of methyl groups for high coverages of ODS and MS, but with CH_2 groups predominating at intermediate chain density. Hexadecane is a linear molecule, expected to intercalate into ODS monolayers and keep the ODS chains well ordered. The highly branched squalane molecule should show little intercalation. Figure 1A indicates that this may be the case. Overall squalane shows lower

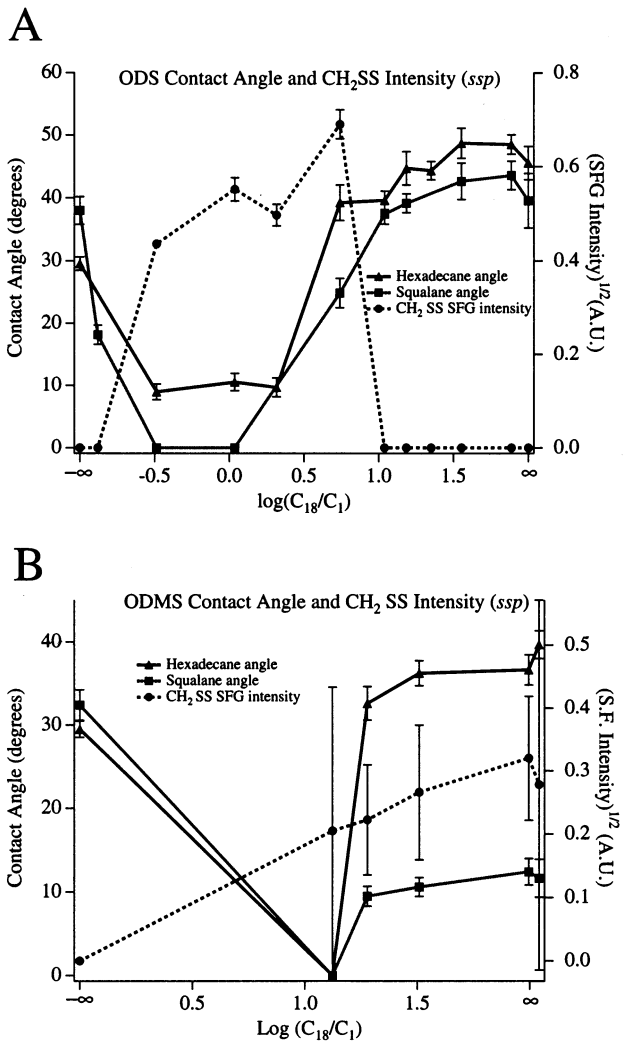

Figure 1. Contact angles of hexadecane, squalane, and CH_2 symmetric stretch peak intensity at the fused silica−air interface: (A) ODS monolayers; (B) ODMS monolayers. Hexadecane contact angles are advancing contact angles; squalane contact angles are static angles.

contact angles than hexadecane, with the greatest difference occurring on surfaces with $\log(C_{18}/C_1)$ values lower than 1.0. Water contact angle measurements decrease steadily from 112.7° to 86.6° for surface composition varying from ODS to MS (individual data not shown).

The ODMS−TMS monolayers are significantly different from ODS−MS monolayers. Water contact angles vary from 104° for an ODMS monolayer to 95° for a TMS monolayer (individual data not shown). In Figure 1B the chain straightening effect of hexadecane appears even more pronounced for ODMS monolayers than for ODS monolayers. The TMS surface (no C_{18} chains present, only CH_3 groups) has a hexadecane contact angle of 29°. The ODMS monolayer shows a contact angle of 40°. These contact angles indicate that the ODMS monolayer surface is primarily CH_3 terminated when exposed to hexadecane. Squalane shows contact angles of 32° for TMS and 12° for the ODMS monolayer, indicating that in squalane the surface is primarily composed of higher energy methylene groups. The difference between the values obtained for hexadecane and squalane indicate that ODMS chains may be more susceptible to ordering due to intercalation of long chain hydrocarbons.

Sum Frequency Generation Spectroscopy. Parts A and B of Figure 1 show the correlation between the square root of the CH_2 *ssp* peak intensity at approximately 2850 cm^{-1} for various

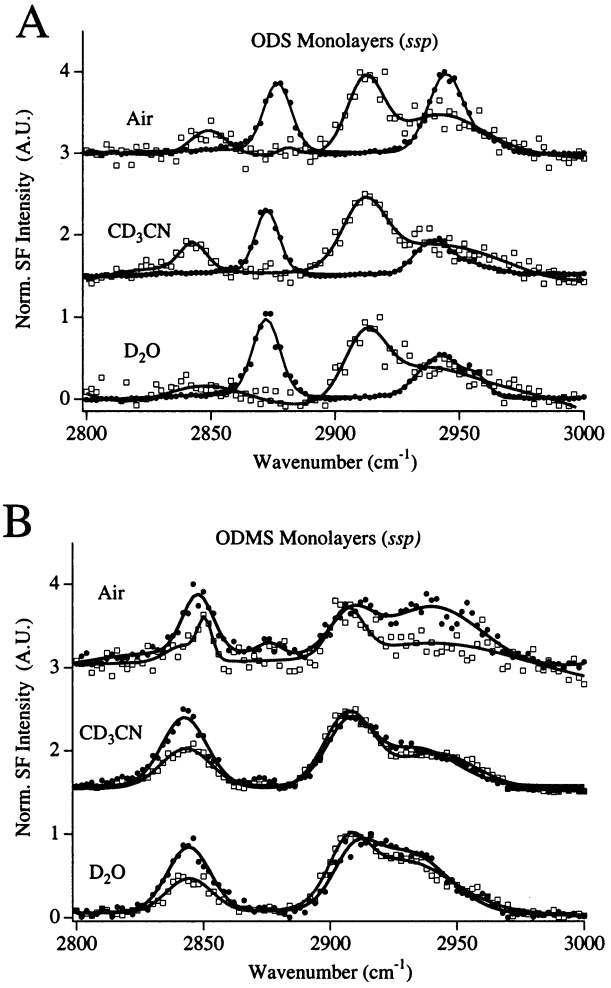

Figure 2. SFG spectra (*ssp*) of ODS and ODMS monolayers in air, CD_3CN, and D_2O. Lines are Gaussian fits to the data. (A) ODS monolayers: (●) 8.0 μmol/m^2, (□) 6.7 μmol/m^2. (B) ODMS monolayers: (●) 4.5 μmol/m^2, (□) 4.4 μmol/m^2).

monolayers in air and contact angles for the monolayers with various probe liquids. The square root of peak intensity is related to alkyl chain density, assuming no change in dipole orientation with changing density. The CH_2 symmetric stretch peak indicates the presence of gauche defects in the chains. This vibrational mode is not SF active when the alkyl chain is in an all-trans conformation due to the near complete cancellation of the nonlinear polarization on adjacent carbons. The intensity of this peak has been successfully used to characterize carbon chain disorder in a variety of systems.[31−33] In this case, CH_2 peak intensity reaches a maximum at alkyl chain densities that produce a minimum in the squalane and hexadecane contact angles for the ODS monolayers. This correspondence indicates that the reduction in contact angles is due to gauche defects in the alkyl chains, which expose a higher energy CH_2 surface to the probe liquid.[33] The data Figure 1B show a consistent, high degree of disorder, as shown by the intensity of the CH_2 symmetric stretch for the ODMS monolayers. At a surface coverage of 4.2 μmol/m^2 this surface is so highly disordered even the CH_2 symmetric stretch peak disappears.

To compare solvent effects on these model chromatographic interfaces, SF spectra were collected in situ, exposed to solvents or air. Parts A and B of Figure 2 show SF spectra of ODMS and ODS monolayers in contact with water, air, and acetonitrile. The most important feature to note in these spectra is the lack of a CH_2 symmetric stretch peak in the 8.0 μmol/m^2 ODS spectra, indicating predominantly an all-trans chain conformation in all solvents. Mixed ODS−MS monolayers, on the other hand, show a strong CH_2 symmetric stretch peak, indicating that for a mixed monolayer of C_1 and C_{18} chains, some gauche defects are present. The SF spectra in Figure 2A shows a spectral shift in the CH_3 symmetric stretch and CH_3 AS peaks. This 10 cm^{-1} shift in the peak position between air and D_2O environments, with D_2O and CD_3CN environments yielding similar peak positions, is consistent with our previous work on ODS monolayers.[34] The SF spectra in Figure 2B show ODMS monolayers in D_2O, air, and CD_3CN at various alkyl chain densities. The spectra are similar, with the dominant feature being the CH_2 symmetric stretch peak. The CH_3 symmetric stretch peak is absent for a 4.4 μmol/m^2 ODMS monolayer in CD_3CN and D_2O, and barely detectable for 4.5 μmol/m^2 monolayer. These spectra show a high degree of disorder in the monolayers studied in all solvent environments. The difference between ODMS spectra in air is probably due to Fermi resonance of the weak CH_3 symmetric stretch peak in the 4.5 μmol/m^2 ODMS sample. The large peak at 2915 cm^{-1} is due to the CH_3 symmetric stretch of the side CH_3 groups of ODMS.

Two types of experiments were performed with ODS and ODMS monolayers to investigate their behavior in various solvent environments. In the first experiment, spectra for the entire range of C_{18} chain densities were collected in contact with pure D_2O, pure CD_3CN, or 90%, 50%, or 10% D_2O-CD_3CN solutions. In the second experiment, the spectra for an ODS monolayer with an alkyl chain density similar to a commercial chromatographic stationary phase was measured in contact with a wider range of CD_3CN-D_2O solution compositions. Binary mixtures of CD_3CN and D_2O in 10% increments by volume were used. Deuterated reagents were used to eliminate any interference from solvent at the fused silica-solution interface.

The graphs in Figure 3A,B show normalized CH_2 symmetric stretch peak intensities for ODS and ODMS monolayers as a function of $\log(C_{18}/C_1)$ ratio in CD_3CN-D_2O solution. In Figure 3A, CH_2 symmetric stretch peak intensities increase as decreasing ODS chain density allows more conformational freedom, then decrease again as the ODS chain density decreases further. For pure D_2O and CD_3CN, the maximum CH_2 symmetric stretch peak intensity is reached at around a $\log(C_{18}/C_1)$ ratio of 0.0 (4.2 μmol/m^2 ODS). The most interesting feature is the variation of intensity with solvent composition. The 50% and 90% D_2O solutions appear to induce more disorder in the alkyl chains than pure D_2O or pure CD_3CN at high chain densities, but the pure D_2O and pure CD_3CN show increased disorder at intermediate chain densities.

The situation is different for ODMS monolayers. In Figure 3B, the CH_2 symmetric stretch peak intensity is shown as a function of the $\log(C_{18}/C_1)$ ratio. The CH_2 symmetric stretch peak intensity decreases with decreasing alkyl chain density, disappearing at a $\log(C_{18}/C_1)$ ratio of 1.2 (3.9 μmol/m^2 ODMS). The intense CH_2 symmetric stretch peak indicates that ODMS is highly disordered, even at infinite $\log(C_{18}/C_1)$ ratio (4.5 μmol/m^2 ODMS). Usually, a decrease in CH_2 symmetric stretch intensity is due to a decrease in gauche defects in the C_{18} chain. In this case, the chains are so disordered that the spatial distribution of gauche defects causes some signal to be canceled. Any ordering of the monolayer will produce an increase in the CH_2 symmetric stretch peak intensity.

Compared to the degree of disorder due to the low packing density of ODMS, solvent-induced disorder effects are minor. All compositions, except pure CD_3CN, show roughly the same

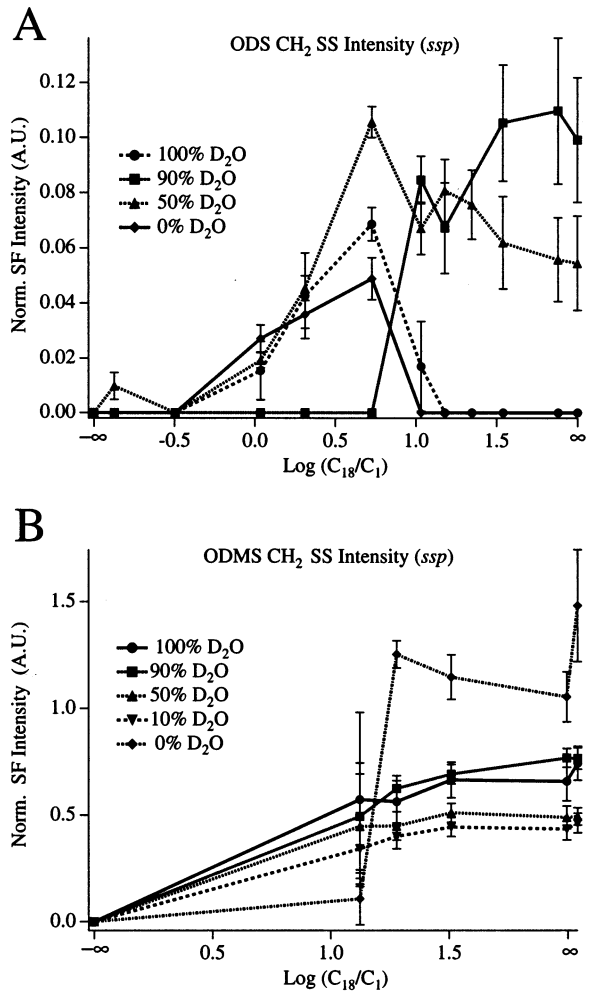

Figure 3. Normalized CH_2 symmetric stretch peak intensity (*ssp*) in CD_3CN-D_2O mixtures: (A) ODS monolayers; (B) ODMS monolayers. Key: (●) 100%; (■) 90%; (▲) 50%; (▼) 10%; (◆) 0%. (All are vol % D_2O.)

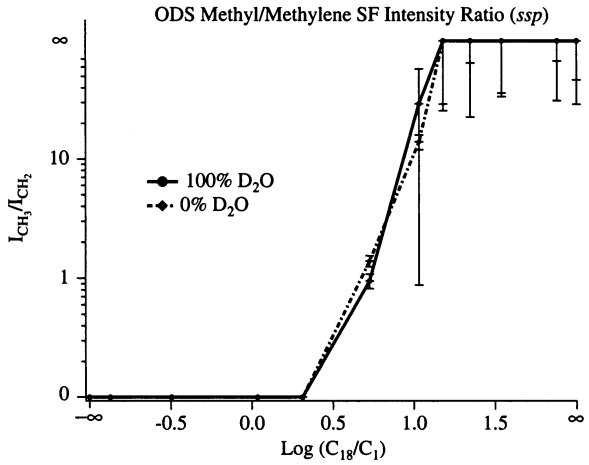

Figure 4. Methyl to methylene peak *ssp* intensity ratios for ODS monolayers in CD_3CN or D_2O solution: (●) 100 vol % and (◆) 0 vol % D_2O). The larger the ratio, the more ordered the C_{18} chains.

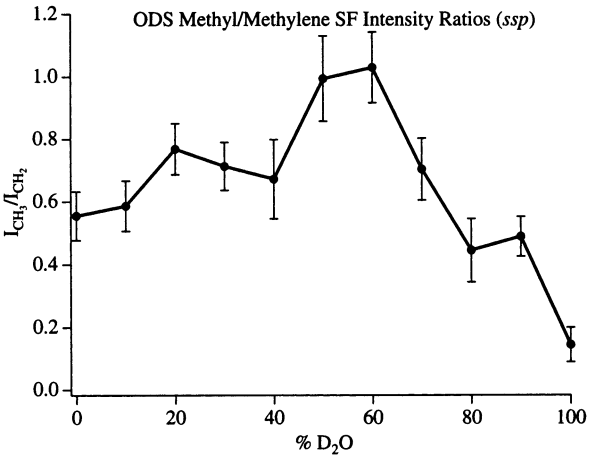

Figure 5. Methyl to methylene *ssp* peak intensity ratios for the 2.2 μmol/m^2 ODS monolayer in CD_3CN-D_2O solution. All solution percentages are in vol % D_2O. The larger the ratio, the more ordered the C_{18} chains.

dependence of CH_2 symmetric stretch peak intensity on alkyl chain density. In CD_3CN, the spectra show a higher CH_2 symmetric stretch intensity than in D_2O or mixed D_2O-CD_3CN solution. On the basis of this increase, it is possible that CD_3CN is actually increasing the degree of order in the monolayer, resulting in the reappearance of the CH_2 symmetric stretch peak.

The effects of chain density and solvent composition on the intensity ratio of the CH_3 symmetric stretch peak to the CH_2 symmetric stretch peak for ODS monolayers are shown in Figure 4. As discussed previously, the I_{CH_3}/I_{CH_2} ratio is a measure of the degree of order present in the chains. The spectra of C_{18} monolayers in contact with pure D_2O and pure CD_3CN are similar, with a high degree of order maintained above a log(C_{18}/C_1) ratio of 1.0 (7.3 μmol/m^2 ODS). Below this density, the monolayer undergoes a transition to a highly disordered state. The error bars shown for the infinite CH_3 symmetric stretch to CH_2 symmetric stretch peak intensity ratios represent the minimum detectable ratio based on the limit of detection for the CH_2 symmetric stretch peak, taken as three standard deviations of baseline noise. The similar behavior of D_2O and CD_3CN indicates that the model systems studied do not collapse when exposed to D_2O.

More detailed data on the effect of solvent on 2.2 and 7.9 μmol/m^2 ODS monolayers were collected. Spectra were collected for 2.2 and 7.9 μmol/m^2 ODS in contact with solutions containing various concentrations of CD_3CN and D_2O. Concentrations varied between pure CD_3CN and pure D_2O in 10% increments by volume. Figure 5 shows the I_{CH_3}/I_{CH_2} ratio as a function of solvent composition for the 2.2 μmol/m^2 monolayer. A change in this ratio is seen at approximately 50−60 vol % D_2O. The spectra of the 7.9 μmol/m^2 ODS monolayer showed a small methylene peak for the 60 vol % D_2O sample, but the intensity was not statistically significant. For the other compositions studied, the 7.9 μmol/m^2 monolayer remained well ordered, with no detectable CH_2 symmetric stretch peak intensity observed (data not shown). In Figure 5, the maximum order occurs around 60 vol % D_2O, corresponding to a CD_3CN mole fraction of 0.2. Previous studies have shown that the excess viscosity and, presumably microheterogenity, of CH_3CN-H_2O solutions peaks at a mole fraction of 0.15.[14] The increase in order of the 2.2 μmol/m^2 monolayer in contact with mixed CD_3CN-D_2O solutions may be due to the microheterogenity of the CD_3CN-D_2O system, possibly indicating a link between microheterogeneity in the bulk solution and monolayer structure.

The position of the CH_3 symmetric stretch peak as a function of D_2O concentration in solution was examined for the 7.9 and 2.2 μmol/m^2 ODS monolayers. The peak position did not vary within the limits of instrumental resolution (2 cm^{-1}) (data not

shown). The I_{ssp}/I_{sps} ratio was examined and found unchanged with changing solution composition for the 7.9 μmol/m^2 sample. This indicates that the CH_3 orientation does not change significantly with composition (data not shown). Due to low signal intensity, adequate *sps* spectra for the 2.2 μmol/m^2 monolayer could not be obtained.

Our results do not indicate that the ODS undergoes a distinct collapse when exposed to solutions of low acetonitrile concentration. In fact, the ODS monolayer shows nearly identical behavior in pure CD_3CN and D_2O. Lack of any spectral evidence indicating collapse of the ODS surfaces may result from several differences between our model system and real chromatographic interphase regions. The first difference may be the lower surface density of alkyl chains on the irregular surface of the silica gel particles. Although flatter than silica gel surfaces, our fused silica substrates are relatively rough, with a RMS roughness of about 1.7 nm, by AFM. Even with some substrate roughness, chain densities are still higher than those found in real chromatographic systems. The second reason a distinct collapse of the ODS surface may not be observed is that the SFG spectra are acquired at ambient pressure, whereas chromatographic separations occur at pressures up to 700 bar. Acetonitrile is in pressure dependent equilibrium between the mobile and stationary phases. The SFG results obtained at atmospheric pressure may not entirely describe the behavior of monolayers at higher pressure.

Summary and Conclusions

Results presented here show that solvent does influence the structure of the stationary phase of mixed $C_{18}-C_1$ composition monolayers. Monolayers formed from polymeric ODS show no discernible differences in chain conformation when placed in CD_3CN or D_2O solutions, in agreement with Raman studies that failed to observe a dramatic collapse of alkyl chains in contact with water.[35] ODMS monolayers show a consistent, high number of gauche defects that are relatively insensitive to solvent composition. When MS or TMS is added to the monolayer as a spacer, obvious changes in alkyl chain conformation occur. Lower chain densities favor gauche defects in ODMS and ODS monolayers. Monolayers composed only of ODMS have a much higher number of gauche defects than those composed only of ODS, due to the lower packing density of ODMS. Even at a maximum surface coverage of 4.5 μmol/m^2 these chains are highly disordered. Monolayers of ODMS in contact with mixtures of CD_3CN and D_2O showed a generally similar level of disorder for 100%, 90%, 50%, and 10% D_2O, but for pure CD_3CN the surface showed some additional order in the chains.

Ordering of the ODS chains as a function of solvent composition was investigated for the CD_3CN-D_2O system. A detailed study of the behavior of high density (7.9 μmol/m^2) and low density (2.2 μmol/m^2 ODS) monolayers with a wider range of CD_3CN concentration indicated that the high-density monolayer is insensitive to solvent effects, but the low-density monolayer showed increased chain order at 50−60 vol % D_2O. Bulk solution microheterogeneity phenomena also reach a maximum at this composition, possibly indicating a link between bulk solvent microheterogeneity and monolayer behavior.

Acknowledgment. This research was supported by NSF (CHE-9875632). The authors acknowledge the allocation of time and services in the Scienta ESCA laboratory of Lehigh University. Professional and technical assistance of Dr. Alfred C. Miller is greatly appreciated.

References and Notes

(1) Alvarez-Zepeda, A.; Barman, B. N.; Martire, D. E. *Anal. Chem* **1992**, *64*, 1978−1984.
(2) DeVido, D. R.; Dorsey, J. G.; Chan, H. S.; Dill, K. A. *J. Phys. Chem.* **1998**, *102*, 7272.
(3) Bliesner, J. M.; Sentell, K. B. *Anal. Chem* **1993**, *65*, 1819−1826.
(4) Thompson, W. R.; Pemberton, J. E. *Anal. Chem.* **1994**, *66*, 3362−3370.
(5) Burns, J. W.; Bialkowski, S. E.; Marshall, D. B. *Anal. Chem* **1997**, *69*, 3861−3870.
(6) Carr, J. W.; Harris, J. M. *Anal. Chem.* **1987**, *59*, 2546−2550.
(7) Pursch, M.; Brindle, R.; Ellwanger, A.; Sander, L. C.; Bell, C. M.; Händel, H.; Albert, K. *Solid State Nucl. Magn. Reson.* **1997**, *9*, 1919−201.
(8) Doyle, C. A.; Vickers, T. J.; Mann, C. K.; Dorsey, J. G. *J. Chromatogr. A* **2000**, *877*, 41−59.
(9) Stalcup, A. M.; Martire, D. E.; Wise, S. H. *J. Chromatogr.* **1988**, *442*, 1−14.
(10) Marcus, Y.; Migron, Y. *J. Phys. Chem.* **1991**, *95*, 400.
(11) Matteoli, E.; Lepori, L. *J. Chem. Phys.* **1984**, *80*, 2856.
(12) Marcus, Y. *J. Chem. Soc., Faraday Trans. 1* **1989**, *85*, 381−388.
(13) Zhang, D.; Gutow, J. H.; Eisenthal, K. B.; Heinz, T. F. *J. Chem. Phys.* **1993**, *98*, 5099−5101.
(14) Davis, M. I. *Thermochim. Acta* **1984**, *73*, 149−164.
(15) Slusher, J. T.; Mountain, R. D. *J. Phys. Chem. B* **1999**, *103*, 1354.
(16) Rutan, S. C.; Harris, J. M. *J. Chromatogr.* **1993**, *656*, 197.
(17) Carr, P. W.; Tan, L. C.; Park, J. H. *J. Chromatogr. A* **1996**, *724*, 1−12.
(18) Wirth, M. J.; Fatunmbi, H. O. *Anal. Chem.* **1992**, *64*, 2783−6.
(19) Wirth, M. J.; Fatunmbi, H. O. *Anal. Chem.* **1993**, *65*, 822−6.
(20) Ohmacht, R.; Kele, M.; Matus, Z. *Chromatographia* **1994**, *39*, 668−72.
(21) Li, L.; Carr, P. W.; Evans, J. F. *J. Chromatogr. A* **2000**, *868*, 153−167.
(22) Hetem, M.; Van de Ven, L.; De Haan, J.; Cramers, C.; Albert, K.; Bayer, E. *J. Chromatogr.* **1989**, *479*, 269−95.
(23) Huang, J. Y.; Shen, Y. R. Sum-Frequency Generation as a Surface Probe. In *Laser Spectroscopy and Photochemistry on Metal Surfaces*; Dai, H.-L., Ho, W., Eds.; World Scientific: Singapore, 1995; pp 5−53.
(24) Fadeev, A. Y.; McCarthy, T. J. *Langmuir* **1999**, *15*, 3759−3766.
(25) Semal, S.; de Ruijter, M. J.; DeHuit, J.; De Coninck, J. *J. Phys. Chem. B* **1999**, *103*, 4854−4861.
(26) Pizzolatto, R. L.; Yang, Y. J.; Wolf, L. K.; Messmer, M. C. *Anal. Chim. Acta* **1999**, *397*, 81−92.
(27) Wang, R.; Wunder, S. L. *Langmuir* **2000**, *16*, 5008−5016.
(28) Nyburg, S. C.; Lüth, H. *Acta Crystallogr.* **1972**, *b28*, 2992.
(29) Wirth, M. J.; Fairbank, R. W. P.; Fatunmbi, H. O. *Science* **1997**, *275*, 44−47.
(30) Yang, Y. J.; Pizzolatto, R. L.; Messmer, M. C. *J. Opt. Soc. Am. B* **2000**, *17*, 638.
(31) Bain, C. D. *Langmuir* **1994**, *10*, 2060.
(32) Messmer, M. C.; Conboy, J. C.; Richmond, G. L. *J. Am. Chem. Soc.* **1995**, *117*, 8039−8040.
(33) Guyot-Sionnest, P.; Hunt, J. H.; Shen, Y. R. *Phys. Rev. Lett.* **1987**, *59*, 1597−1600.
(34) Wolf, L. K.; Yang, Y. J.; Pizzolatto, R. L.; Messmer, M. C. Microscopic Structure of Chromatographic Interfaces as Studied by Sum-Frequency Generation Spectroscopy. In *Interfacial Properties on the submicrometer scale*; Frommer, J., Overney, R. M., Eds.; American Chemical Society: Washington, DC, 2001; Vol. 781, pp 293−305.
(35) Doyle, C. A.; Vickers, T. J.; Mann, C. K.; Dorsey, J. G. *J. Chromatogr. A* **1997**, *779*, 91−112.